

PROCEEDINGS OF SPIE

[SPIDigitalLibrary.org/conference-proceedings-of-spie](https://spiedigitallibrary.org/conference-proceedings-of-spie)

New liquid crystal materials enabling revolutionary display devices

Julia Anne Kornfield, Noel A. Clark, Larry Dalton, Seth R. Marder, Christopher Kemper Ober, et al.

Julia Anne Kornfield, Noel A. Clark, Larry Dalton, Seth R. Marder, Christopher Kemper Ober, Peter Palfy-Muhoray, Joseph W. Perry, Ned Thomas, David M. Walba, Shin-Tson Wu, "New liquid crystal materials enabling revolutionary display devices," Proc. SPIE 4712, Cockpit Displays IX: Displays for Defense Applications, (28 August 2002); doi: 10.1117/12.480960

SPIE.

Event: AeroSense 2002, 2002, Orlando, FL, United States

New liquid crystal materials enabling revolutionary display devices

Julie Kornfield, California Institute of Technology (Director, AFOSR Liquid Crystals MURI 1997-2001); Noel A. Clark, University of Colorado; Larry Dalton, University of Southern California; Seth Marder, University of Arizona; Chris Ober, Cornell University; Peter Palffy-Muhoray, Kent State University; Joseph W. Perry, University of Arizona; Ned Thomas, Massachusetts Institute of Technology; David M. Walba, University of Colorado; Shin-Tson Wu, University of Central Florida.

ABSTRACT

The Display and Beam Steering Thrust of the AFOSR Liquid Crystal MURI addressed key materials and device technology issues affecting performance of liquid crystal (LC) electro-optic (EO) devices, particularly device structures useful in information *Displays* and for *Laser Beam Steering and Switching*. Two basic themes were development of bulk LCs having high performance characteristics (nematic LCs, and chiral smectic LC devices having analog response), and development of novel LC electro-optic structures. Research on novel device structures led to advances in LC alignment and on photonic band-gap materials.

Keywords: analog FLC, LC elastomers, LC gels, LC block copolymers, organic laser, photobuffing, NLO, LC gratings

1. TECHNICAL HIGHLIGHTS FROM THE MURI EFFORT IN LC ELECTRO-OPTICS

1.1. V-shaped Switching in Tilted Chiral Smectic Liquid Crystals

Thresholdless switching has been observed in specially developed chiral smectic liquid crystals. Display cells utilizing these materials show a nearly linear dependence of optic axis orientation on applied voltage. Space charge effects screen the electric field in the liquid crystal, and “stiffening” of the polarization causes the material to orient as a uniform whole. The detailed understanding of this underlying mechanism, which has been gained under this MURI, opens the door to the construction of a new generation of grayscale active matrix liquid crystal displays with high contrast and vastly improved response times.

1.2. Mirrorless Lasing in Cholesteric Liquid Crystalline Materials

Due to their inherently periodic structure, cholesteric liquid crystals are one-dimensional photonic band-gap materials. In addition to their utility as switchable mirrors for beam steering applications, optically pumped thin cholesteric liquid crystal films, either low molecular weight liquids or liquid crystal polymers, can simultaneously act both as the distributed cavity host and the active medium, and emit laser radiation at the reflection band edge. Such films can enhance the emission spectrum and directionality of backlights for liquid crystal displays, and serve as organic thin film low threshold tunable laser light sources. Liquid crystalline elastomers are particularly interesting, since the reflection band edge and hence the lasing wavelength can be tuned by stretching the elastomer sample. Cholesteric elastomers can therefore act as tunable laser sources, as well as elements for remote sensing.

1.3 Brownian Ratchet Mechanism in Photobuffing of Liquid Crystal Alignment Layers

Optically induced anisotropy in photosensitive alignment layers has been shown to effectively align liquid crystals. In addition to overcoming problems associated with conventional mechanical rubbing, photobuffing allows spatially and temporally varying liquid crystal alignment. Understanding the underlying “orientational ratchet” mechanism, where light effectively exerts a torque on the material without the transfer of angular momentum, allows accurate control of the alignment layer anisotropy and subsequent liquid crystal alignment. In addition to use in the manufacture of flat panel displays, photobuffing enables the implementation of liquid crystal technology on curved plastic substrates, such as switchable/tunable filters and polarizers for eye protection, and ambient light control elements for the visors of helmet mounted displays.

1.4 Optomechanical Response of Nematic Liquid Crystal Elastomers

Liquid crystalline elastomers are mesogen containing rubbers, characterized by coupling between orientational order and mechanical strain. In addition to changing their optical properties when subjected to mechanical deformations, changing the order parameter of these materials results in strain and a change of macroscopic conformation. A particularly efficient method of changing the order parameter is by light. Illuminating dye containing liquid crystal elastomers can dramatically change the order parameter, and result in large and rapid changes in shape of the sample. The coupling allows a new way of changing the orientational order, resulting in a new mechanism for the optomechanical response, making these materials ideal candidates for a variety of applications as optomechanical actuators, artificial muscles and adaptive optical elements.

2. ACCOMPLISHMENTS/NEW FINDINGS

2.1 Dopants and NLO Dyes: University of Arizona

Marder and **Wu** have collaborated to develop a series of colorless, high dielectric anisotropy dopants for lowering the operational voltage of LC compositions. These new dopants are significant in a wide range of electro-optic devices spanning displays, beam steering and laser hardening. A joint Caltech/Hughes patent has been filed on these materials.

Two-photon dyes have been synthesized by **Marder**; characterization of these has been performed by **Perry** and **Palfy-Muhoray**. Among other applications, two-photon dyes are of potential interest in photoalignment, since they allow high spatial resolution, two-beam writing, and a sharper writing threshold. A new two-photon azo-dye YZAZO5 has been synthesized with the structure shown below.

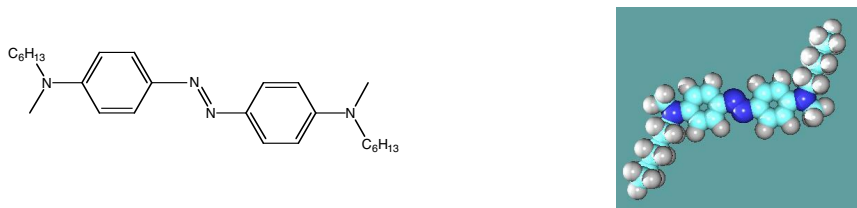


Figure 1. The composition and structure of YZAZO5.

Preliminary work in the optical characterization and photoalignment properties of films with YZAZO5 has been carried out at Kent State. The emission and excitation spectra are shown in Fig. 2. Photoalignment layers were prepared with this dye, and laser writing has been demonstrated in a nematic cell filled with E7. The photosensitivity of the alignment layer is extremely high, enabling writing with pump powers as low as 2 mW.

Marder has synthesized a new class of disk-like mesogens for electron transport applications. Work on characterizing a series of these compounds has recently been started in collaboration with the groups at Kent, Colorado and Caltech.

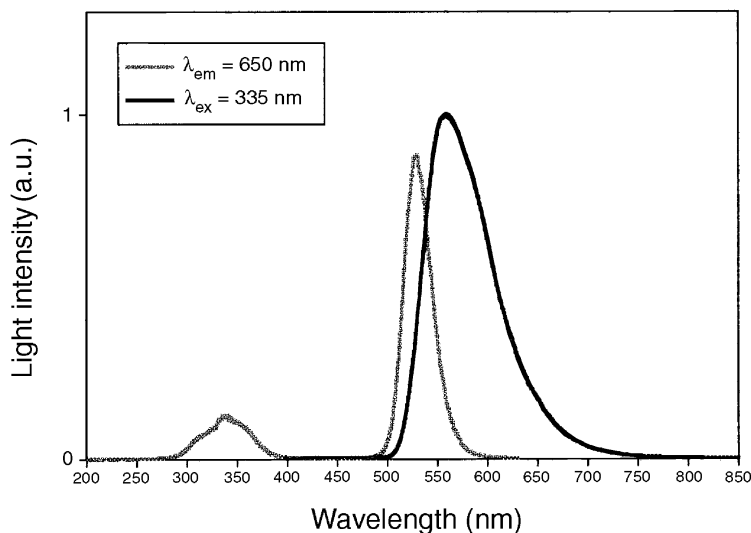


Figure 2. Emission and excitation spectrum of YZAZO5.

2.2 Reversible LC Gels with Exceptional Uniformity: California Institute of Technology

LC elastomers are of interest for diverse applications from actuators and sensors to responsive optical elements. Systematic control of the coupling between the mechanical and optical responses of the materials is needed to improve attributes from the sharpness of their mechanical response to stimuli (temperature, light or electric fields) to the uniformity of their optical properties. Therefore, the MURI team has developed synthetic methods to prepare polymers that self-assemble gels in LC solvents. Because the polymer molecules may be dissolved and characterized, the length of the strands between crosslinks in the physical gel is well defined. By pushing out the limit in the length of side-group liquid crystal polymers that can be prepared by polymer analogous synthesis, this research opens the way to highly uniform liquid crystalline gels with lower polymer concentrations (hence faster electro-optic response) than have been accessible previously. The efforts in the **Kornfield** group are highly collaborative, with input from the **Ober** group in optimizing the synthesis, from Shin-Tson **Wu** at Hughes in electro-optic measurements and from Noel **Clark** and Dave **Walba** on molecular design of FLC gels and their characterization.

Our initial physical studies have examined nematic solutions and gels. **Kornfield** and **Ober** extended polymer analogous synthesis to produce very high molecular weight ($\sim 1 \times 10^6$ g/mol) side group liquid crystalline polymers (SGLCPs). Solutions of SG-LCP homopolymers have been used to establish the concentration dependence of key liquid crystal properties for electro-optic applications (order parameter, elastic and viscous constants, phases and transition temperatures). Rheo-conoscopy has been employed to observe the effect of low concentrations (<10%) of ultra-long SG-LCP on the orientational response of a low molar mass LC host. Unprecedented transformations of shear alignment character were induced. We have demonstrated adding ultralong, oblate SGLCP to a nematic host can induce not only the familiar change from flow aligning to tumbling, but can decrease the tumbling parameter so strongly that the material becomes flow aligning again—with the director along the gradient direction! The powerful effect of the polymer on the orientational response of nematics due to flow is demonstrated to be a consequence of the exceptional length of the polymer (Fig. 3). Based on the observed behavior of these nematic solutions, the orientational behavior of nematic gels was accurately predicted. Advances in the SGLCP synthesis were further used to prepare coil-SGLCP-coil block-polymers designed to self-assemble reversible gels in nematic LC solvents. Ultralong SGLCP triblock copolymers were shown to form highly uniform, self-assembled LC gels. Using very long SGLCP midblocks (~ 1 M g/mol) provided homogenous, single-phase gels with relatively low polymer concentrations ($\sim 15\%$ in 5CB of a triblock with 50k PS end blocks and a 1.9M SGLCP midblock with CB side groups). Small applied strain causes the director to align with such uniformity that a conoscopic figure is readily observed (Fig. 4). To our knowledge, no other route to LC gels provides access to this level of optical uniformity. Electro-optic switching is observed, with threshold voltage increased approximately six fold relative to pure 5CB.

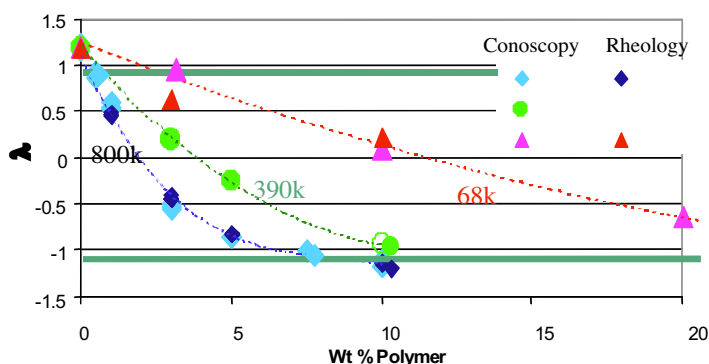


Figure 3. Ultra-long SGLCP shows exceptionally strong effects on the orientational response of the host LC (PBCB6 dissolved in 5CB at 25°C). The observation of a tumbling parameter more negative than -1 is unprecedented; it indicates that the mild orientation of low-concentrations of the 800k g/mol PBCB6 effectively commands the orientation of the director, causing it to align nearly along the velocity gradient direction (perpendicular to the shear alignment direction of all prior flow-aligning calamitic nematics). The effect of SGLCP molecular weight on the effect shows that this behavior is indeed due to the exceptionally high molecular weight we have been able to reach: when the chain length is lowered to the range that has been examined previously (≤ 100 kg/mol), the effects of added polymer are relatively modest, in accord with prior literature.

In addition to potential applications in roll-to-roll processable LC displays, the nematic gels have potential for “artificial muscles” with sharper thermal transitions than existing LC elastomers. The self-assembly strategy for forming LC gels and using them to align LC phases can now be extended to cholesteric and smectic LCs, including the deVries smectics that exhibit V-shaped switching and the chiral smectic banana phases, neither of which can be aligned by any current method.

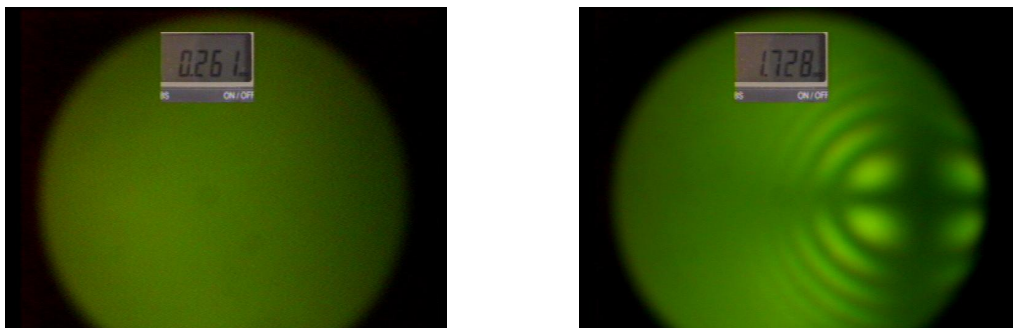


Figure 4. Conoscopic image: left, an unaligned sample of gel; right, the same sample subjected to 100% shear strain. The formation of an interference figure indicates that the director field and order parameter are highly uniform throughout the specimen, a signature of the highly uniform network structure formed by self-assembly. The position of the center of the interference figure indicates that the director is oriented nearly along the gradient direction, as anticipated by the observation of a tumbling parameter more negative than -1 (Figure 3).

2.3 Analog FLCs and Smectic Polymers for NLO Fiber Optics: University of Colorado

Emphasis at Colorado has focused on synthetic (**Walba**) and physical (**Clark**) studies of analog electro-optic effects in ferroelectric liquid crystals, and on a novel liquid crystalline material for optical fibers for non-linear optical applications. The former is directed at the design of a new generation of analog chiral smectic displays, while the aim of the latter is toward ferroelectric liquid crystal nonlinear optic fibers with a photonic bandgap. In addition to studying and characterizing alignment layers produced by **Palfy-Muhoray**, a new effort has started in carrying out photobuffing at Colorado to enable the realization of bookshelf textures using photoalignment techniques.^[1]

Due to the MURI, emphasis on analog EO modulation for optical beam steering and displays, one a key project in the Boulder MURI labs has been studies on the origins of the very high susceptibility analog modulation achievable in “thresholdless antiferroelectric” FLC devices. Recent work from the **Clark** labs has shown that all of the considerable literature in the field has been mistaken. The analog, so called “V-shaped switching” does not have anything to do with antiferroelectricity.^[2]

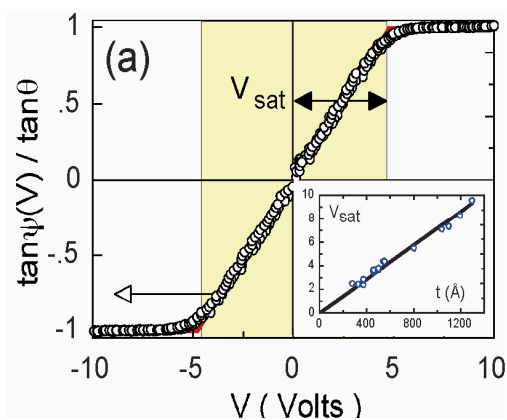


Figure 5. E-field-induced rotation of the optic axis in a SmC* analog SSFLC cell. Sufficiently high polarization and sufficiently thick insulating alignment layers combine to make the cell exhibit analog EO, with a saturation voltage V_{sat} that depends on the alignment layer thickness, t (inset).

Rather, this valuable effect occurs in SmC* cells with special alignment conditions. Of particular importance is the insulating character of the alignment layers, which enable the reorientation of the SmC* polarization to completely screen applied electric field.^[3] The Boulder group insights into the origins of the effect have already led to the discovery of new V-shaped switching materials^[4] with extremely promising properties for incorporation into beam-steering devices, among others.

A main-chain NLOP of sideways-dimer mesogenic units (negative birefringence) which can be pulled into robust fibers where the polarization is normal to the fiber axis, has been synthesized by **Walba** using ADMET polymerization of a mesogenic diene. X-ray diffraction shows that the smectic layering is highly ordered with the layer normal parallel to the fiber axis. This enables a detailed understanding of the LC structure of the fibers.^[5]

2.4 Hydrogen Bond Attachment of Side-Groups to SGLCP Block Copolymers: Cornell University

Block copolymers are gaining more and more attention both for fundamental research and for industrial applications due to their nanoscale microstructures and the capability of combining many desired properties into a single molecule. The side-group modified liquid crystalline block copolymers (SGLCBCP) have been investigated recently not only because of their specific microphase structures but also the advanced applications made possible by liquid crystallinity, for example, microphase stabilized ferroelectric liquid crystals. Though the covalently bonded SGLCBCPs possess interesting properties, there are still limitations due to their complex synthesis and the slow response. Instead, *hydrogen bonding* may offer an easier way to modify composition and the possibility of increasing the switching response speed since the hydrogen bonds are strong enough to form stable links between the polymer backbone and the side groups, but not so strong as to hinder mobility of the side groups. This approach provides a route to fine-tune the volume ratio between the two blocks by addition of the desired amounts of side groups and to tune the properties (e.g. refractive index) of the LC block by adding the additional moieties. The combination of a periodic nanostructure and liquid crystallinity offers us an exciting approach to make photonic band gap (PBG) materials that could be very useful in the communication industry.

To accomplish our goal for making compositionally tunable photonic bandgap (PBG) materials in the visible (VIS) and near IR ranges, **Ober** used high molecular weight poly(styrene-*block*-acrylic acid) as the polymer backbone with poly(acrylic acid) block functions as the proton acceptors and the side groups with imidazole or pyridine groups at one end of the mesogenic molecules as the proton donors. For the polymers, we have already synthesized P(S-*b*-AA) with several different molecular weights via the hydrolysis of anionically polymerized poly(styrene-*block*-*t*-butylacrylate). The very high MW P(S-*b*-tBA) [310K-115K] film shows blue color and a lamellar morphology, which means this MW is high enough to form a PBG film in the VIS wavelength range after modification of the polymer. Narrow MWD of the polymer is important for the formation of desirable periodic structures or morphologies, otherwise, the PBG properties won't be observed even for high MW polymers. To prove the H-bonded SGLCBCP is a homogeneous system without macrophase separation and periodic nanostructure after blending of polymer backbone and mesogens, we started from the simple mesogen (Fig. 8) and smaller MW P(S-*b*-AA).

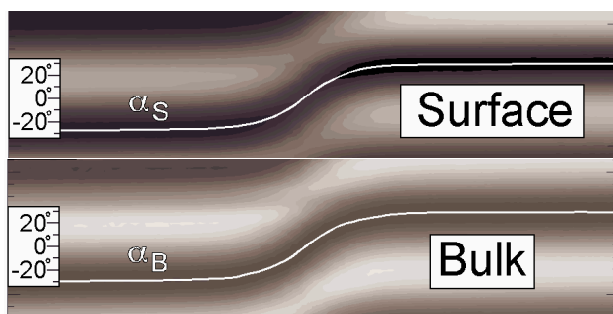


Figure 6. In this regime, bulk and surface molecular orientation, measured respectively by polarized transmission and reflection optical microscopy, are essentially identical, evidence for the polarization charge stiffening of the molecular orientation field. Clark's electrostatic model accounts for these observations.

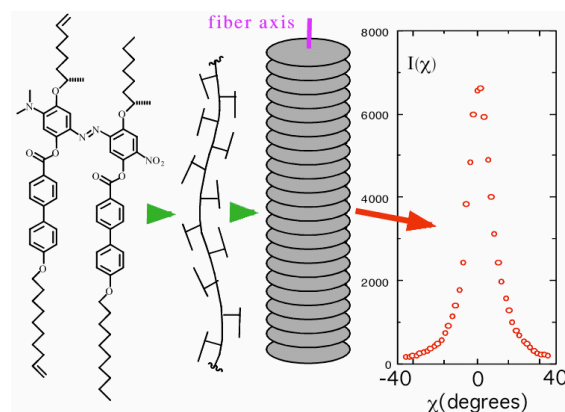


Figure 7. Main chain polymer of chiral side-by-side twins connected by a relatively high β azo group. The oligomers of this material can be pulled into fibers of a few μm diameter, which x-ray diffraction shows have smectic layers well aligned normal to the fiber axis. The layer spacing indicates that the phase is a SmC*.

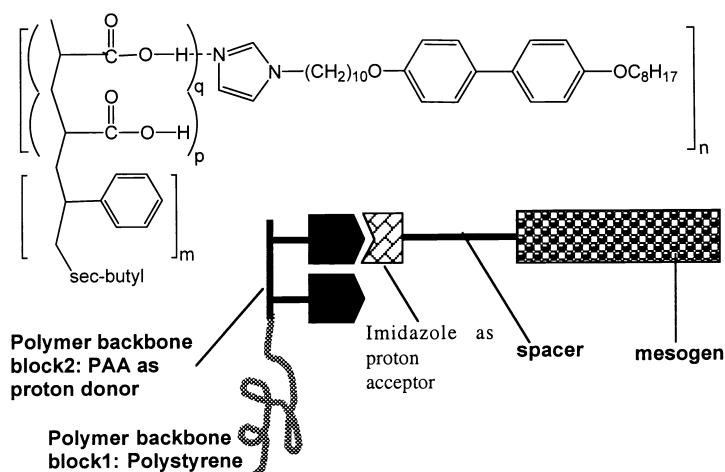


Figure 8. Chemical structures and components of H-bonded SGLCBCP.

Polarized optical microscopy and DSC studies prove the homogeneity of the blends with several different blend ratios while TEM studies show the high regularity of the morphology.

Moreover, we observed that the blend may form some complex morphologies such as H-bonded layers located in lamellae (Fig. 9) which was not seen in covalently bonded SGLCBCP systems. However, as polymer MW goes up, immiscibility increases, and the blends have a tendency to macrophase separate when the blend ratio (side group/acid group on the backbone) is larger than 0.8. To approach a primary goal of the project, an electric field switchable PBG mirror, the mesogens have been designed to

possess strong dipole moment. Molecules having chiral centers or cyano groups have been synthesized and the switching study of the blend of PAA homopolymer and the mesogens is under investigation. Recent results show it is indeed possible to electrically switch the photonic bandgap properties of these blends using AC electric fields.

2.5 Control of Alignment and Band-Gap Structures in LCs:

Kent State University

The main efforts during the MURI have been directed at understanding

1. the dynamics of photoinduced reorientation and photobuffing
2. mirrorless lasing in cholesteric liquid crystalline materials, and
3. the study of the optomechanical response of liquid crystalline elastomers.

Both experimental and theoretical work has been carried out by **Palffy-Muhoray** to probe the mechanism of light induced reorientation in liquid crystals. This included the measurement of optical nonlinearities in dyed liquid crystals, and the measurement photoinduced anisotropy in photosensitive alignment layers. The results were interpreted in terms of a generalized Fokker-Planck model.

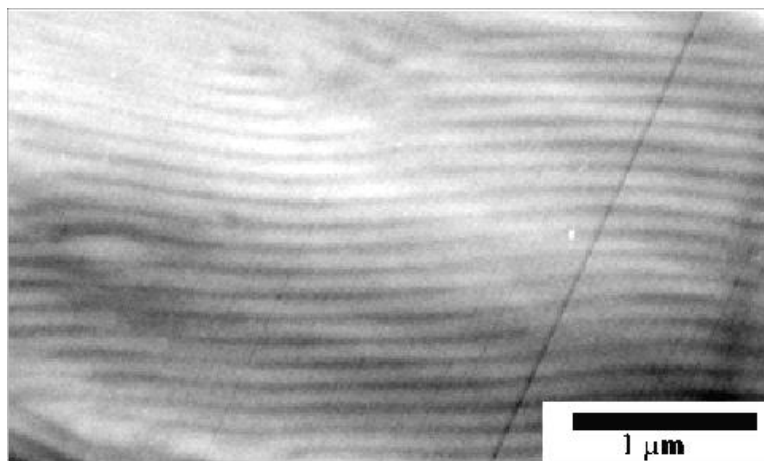


Figure 9. TEM image (Thomas) of one-dimensional lamellar morphology of P(S-b-MAA)/0.60M LC. The dark areas correspond to the MAA-LC domains.

Cholesteric liquid crystals are self-assembled photonic band-gap materials. The band structure gives rise to distributed cavity effects which allow population inversion in optically pumped samples, and mirrorless lasing. Fluorescent emission and lasing have been studied in low molecular weight liquid crystals, and in free standing liquid crystalline polymers and elastomers.

Recently, the optomechanical response of liquid crystalline elastomers has been studied. The dynamic response of azo-dye doped nematic elastomers has been characterized as function of irradiation intensity, wavelength, and dye concentration. The anomalous photoinduced reorientation of dye-doped liquid crystals, where light reorients the director against an elastic restoring torque essentially without the transfer of angular momentum, has presented a formidable

puzzle to our understanding of light-matter interactions. Understanding the underlying mechanism is not only essential to our fundamental understanding, but is of key importance for the effective photobuffing of alignment layers needed in displays and other liquid crystal electrooptic devices.

It has been shown by the Kent group that the reorientation occurs via an orientational Brownian ratchet mechanism, where the dye molecules act as rotors of a light-driven molecular motor^[6]. The process can be modeled via a Fokker-Planck description, comparison of experiment and simulation is shown below.

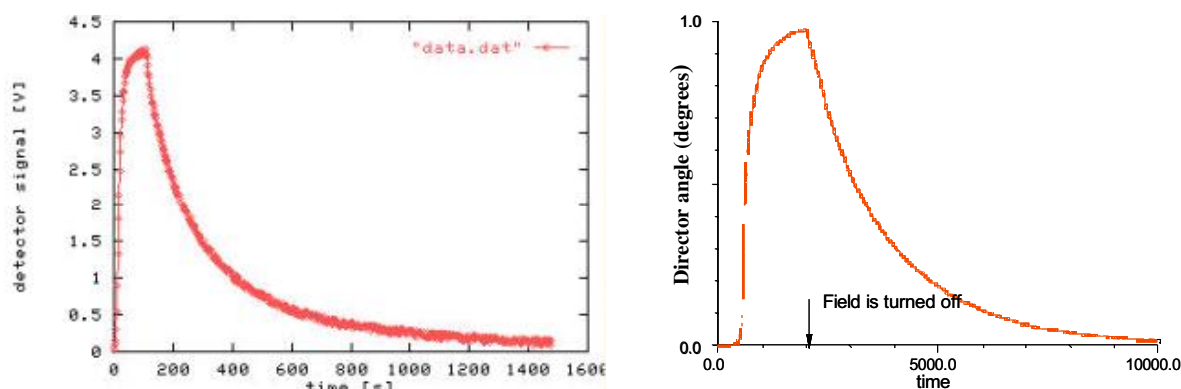


Figure 10. Onset and decay of photoinduced twist: experiment and simulation.

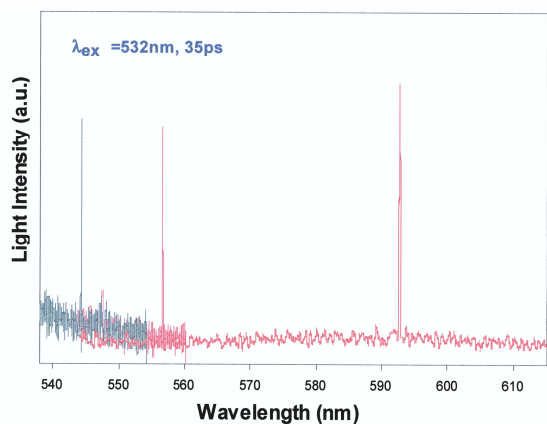
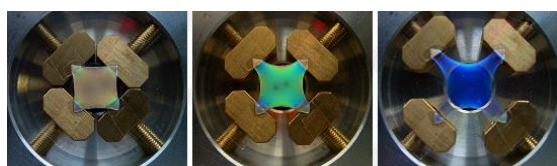


Figure 11. Cholesteric elastomer under biaxial stretch. The colors show the shift of the reflection band above, the shift of laser lines is shown below.

Together with **Clark**, information has been obtained on the orientational distribution function of the photoaligned dye^[7]. Photoalignment has also been demonstrated in alignment layers incorporating the new two-photon azo-dyes from **Marder**.

Cholesteric liquid crystals are periodic dielectric structures and hence self-assembled photonic band-gap materials. Due to distributed cavity effects, in optically pumped samples, population inversion can occur, and above a threshold, mirrorless lasing. The Kent group has unambiguously demonstrated mirrorless lasing, for the first time, in samples of low molecular weight liquid crystals, in free standing liquid crystalline polymer films and in liquid crystalline elastomers^[8]. The observed thresholds are typically low, in the nJ range, with linewidths of 3Å and light to light efficiency near 20%. Since the optical properties of liquid crystalline elastomers can be changed by mechanical strain, lasing can be tuned by stretching these samples. The shift of the reflection band and of the laser line at the band edge in a cholesteric liquid single crystal elastomer is shown in Fig. 11.

Liquid crystal elastomers are exciting new responsive materials, whose physical properties are greatly influenced by the coupling between mechanical strain and orientational order. Changing the order parameter in these materials results in mechanical strain and change in the macroscopic configuration. The order parameter may be changed if the

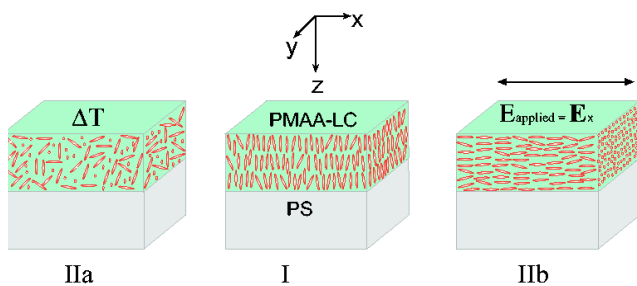


Figure 12a

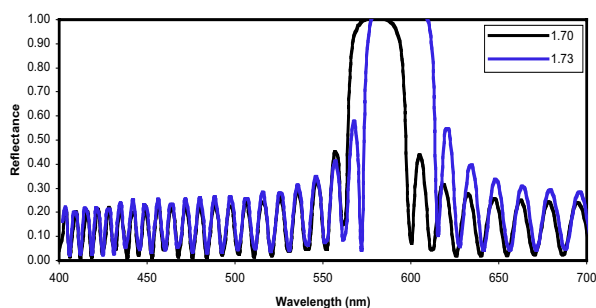


Figure 12b

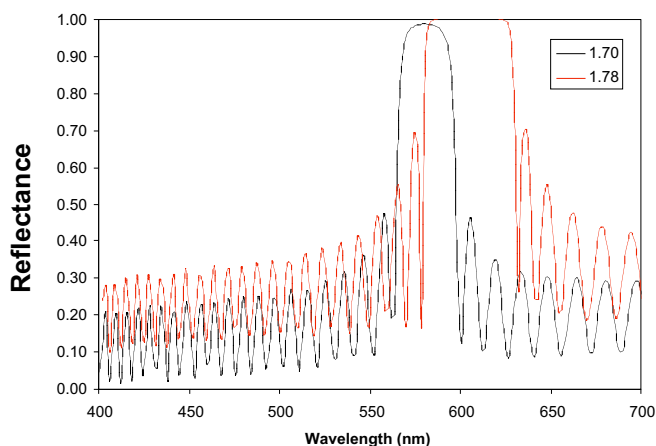


Figure 12c

by approximately 10 nm for a change of 50°C (Fig. 15). From simulations it is possible to identify relevant criteria (refractive indices, mesogen orientation, anchoring conditions and microdomain geometry) that are useful in the design of LC-BCP material systems to achieve particular optical properties.

In addition to the need to provide a large difference in the respective dielectric constants of the materials comprising the photonic crystal, it is highly desirable to utilize materials whose index of refraction may be tailored and thus afford tunable photonic crystals. Several approaches to tunability have been explored, one route is to use optical pumping to create free charge carriers in a semiconductor^[9], another is to trigger a change in the lattice spacing of a colloidal crystal

sample is irradiated by light; either due to heating due to absorption, due to a direct optical torque on the mesogens, or by an indirect optical torque via a ratchet mechanism. Very recently, the optomechanical response of nematic elastomers doped with an azo dye has been studied. Under laser illumination, the elastomer samples showed remarkable large mechanical deformations on very fast timescales.

2.6 Responsive Photonic Band-Gap Materials LC Block-Copolymers: MIT and Cornell

The main objective was to fabricate a self assembled tunable optical switch in the visible using block copolymers with side chain liquid crystalline blocks. This task built upon the knowledge gained in the early years of the MURI in learning how to control the morphology of liquid crystalline polymers and on an understanding of simple 1D periodic optical systems. Hydrogen bonding was used to deliberately induce the formation of a liquid crystalline mesophase in one block of a suitable coil-coil diblock copolymer host. The incorporation of liquid crystallinity in a block copolymer results in an active material that can be used in electro-optic devices. As described above, **Ober** synthesized using anionic polymerization and hydrogen bonding a side group liquid crystalline diblock copolymer (LC-BCP) with a temperature dependent, limited photonic band gap in the visible. The P(S-b-MAA/LC) self assembles by simple solvent casting into a 1D lamellar microdomain structure with a 175 nm period (Fig. 13). The as-formed structure exhibits an optical stop band in the green (Fig. 14a). Tunability of this structure is then shown by thermally inducing changes in the refractive index of the LC layers via alteration of the order parameter of the mesogens. The center of the stop band can be reversibly red shifted

gel by for example, pH, temperature, ionic strength etc^[10, 11], another is to mechanically deform the lattice^[12], and another is to infiltrate the photonic crystal with a liquid crystal^[13-16]. Both heat and electric fields can be used to dynamically manipulate the index contrast presented to incident polarized light by a periodic LC BCP photonic crystal. For initial work, we chose the simplest microdomain structure, namely the 1D periodic lamellar structure with alternating layers in our case of poly(styrene) and poly(methacrylic acid-LC), with the LC-containing layers displaying a smectic structure with homeotropic boundary condition as depicted schematically in structure I of Fig. 12a. Poly(styrene) is isotropic with an index in the visible of 1.59, poly(methacrylic acid) is also isotropic with an index of 1.45 and the imidazole mesogen is assumed to be uniaxial with an index of 1.80 in the isotropic regime. Thus, at temperatures below the smectic to isotropic transition, light incident along z, polarized along x, experiences an index of $n_A = n_{PS}$ in the poly(styrene) layers and $n_B = \left(\varphi_{LC} n_o^2 + (1 - \varphi_{LC}) n_{PMMA}^2 \right)^{1/2}$ in the poly(methacrylic acid-LC) layers where n_{PMMA} is the index of the poly(methacrylic acid) backbone and n_o is the ordinary refractive index of the mesogens. On thermal clearing of the LC, the sample will have morphology as depicted in structure IIa. For reasonable values of birefringence for the organic mesogen, $\Delta n = n_e - n_o \sim 0.07 - 0.20$, we can expect a change in the index of B layers in the system upon thermal clearing of the liquid crystalline state of roughly $\Delta n_B = n'_B - n_B \sim 0.02 - 0.05$ for $\varphi_{mesogen} \sim 0.7 - 0.8$. Calculations using the Berreman transfer matrix method^[17] for a 50 bi-layer stack predict a broadening and shifting of the stop-band towards the red with a corresponding increase in the reflectivity (Fig. 12b). Alternatively, the index can be changed via an applied electric field by reversibly aligning either the ordinary or extraordinary components of the mesogen's refractive index parallel to the oscillation of the electric field of the incoming light. Assuming a positive dielectric susceptibility, an applied electric field \vec{E}_x could realign the mesogens along the x-axis so that for incoming light with electric field vector oscillating along x (structure IIb), the index in the B layers is now given by $n''_B = \left(\varphi_{mesogen} n_e^2 + (1 - \varphi_{LC}) n_{PMMA}^2 \right)^{1/2}$. In this case, a greater effect would be produced, $\Delta n_B = n'_B - n_B \sim 0.06 - 0.16$, using the same range of values for the mesogen birefringence (Δn) and volume fraction ($\varphi_{mesogen}$) given above (Fig. 12c). The typically high electric fields (30-300 V/ μm) necessary for LC reorientation are usually realized with reasonable voltages by using a thin sample. However, the inherently layered geometry with homeotropic anchoring of the mesogens in our present material requires that a potential difference be placed across the usually large sample dimension along the x direction. In our initial experimental work, we pursued the thermal approach to index manipulation.

A P(S-b-AA) diblock copolymer having a 500k g/mol PS block and a 96k g/mol PMAA block was synthesized as described above and blended varying amounts of the H-bonding mesogen to form the SG-BCP (Fig. 8). Films were cast from solution at 2-5 wt.% in THF. Solvent removal was conducted by evaporation over 18 hours at room temperature (22-24 °C) in a THF vapor saturated atmosphere to produce films approximately 5 microns to 200 microns thick. Films were subsequently dried under vacuum for 12 hours. The films were characterized thermally using differential scanning calorimetry (DSC) and optically using polarized optical microscopy (POM) and transmission/reflectance spectrophotometry. Microstructures were observed using small angle x-ray scattering (SAXS), and transmission electron microscopy (TEM).

The neat diblock copolymer, P(S-b-MAA) forms hexagonally packed cylinders of poly(methacrylic acid) embedded in a poly(styrene) matrix, as deduced by TEM and SAXS. The average cylinder-cylinder spacing was 120 nm and simple cast films of the polymer are clear and colorless. The mesogen is a white powder with a melting point of 46 °C. It is approximately 30 Å in length and found by SAXS to have a layer period of 54 Å, suggesting a partially interdigitated bilayer arrangement.

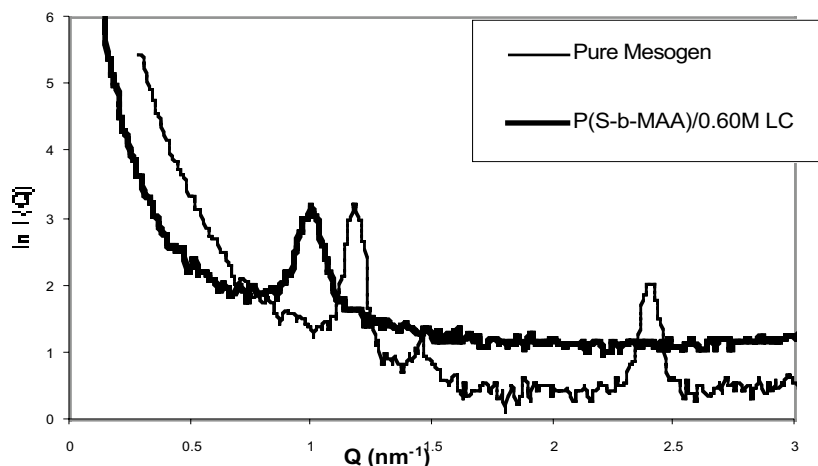


Figure 13. SAXS from P(S-b-MAA)/0.60M LC and the pure mesogen.

P(S-b-MAA) forms single-phase films over the composition range studied, from 0.10 to 0.80 molar ratio of mesogen to acrylic acid repeat units. SAXS and DSC confirmed the formation of a liquid crystalline phase within the block copolymer that exhibited distinctive structural and thermal characteristics as compared to those of the pure mesogen. The smectic to isotropic transition in the LC-BCP occurs over a broad temperature range, from about 65-85 °C. The heat of transition (normalized to the LC block content) on the

initial heating is 10.7 J/g whereas it is 3.2 J/g on second and subsequent heatings. The disparity in the enthalpies suggests that the first passage through the clearing point involves a transition from an LC structure with a higher degree of order as compared to the second and subsequent transitions. The morphology which is initially established during solvent removal becomes inaccessible to the system during the subsequent thermal cycles in the melt state. The transition enthalpy of 3.2 J/g is on the same order of magnitude as observed in covalently bound systems previously studied^[18]. Thermal treatments below about 110 °C do not appear to cause noticeable macrophase separation of the mesogen from the block copolymer host - there is no evidence of pure mesogen signatures in the DSC and SAXS of samples which have undergone heating up to 110 °C for short times. Beyond 110 °C, accelerating anhydride formation along the methacrylic acid backbone depletes mesogens from the polymer resulting in their macrophase separation from the polymer chain and the production of turbidity in the films.

P(S-b-MAA/LC) films less than 200 microns thick were clear and appeared blue to green depending on the particular LC content and the viewing angle. In particular, at 0.60 molar ratio (0.60M) and for normal incidence, green films were produced, as shown in the photograph in Fig. 14a. Heating into the isotropic regime gives a film with red-orange color in reflection (Fig. 14b). Bright field TEM images of cross sections of the films (see Fig. 9) indicate that the LC BCP self-assembled into a lamellar structure, with a layer period of approximately 165 nm with the lamellae preferentially oriented parallel to the surface of the glass vial in which the samples were cast. The dark areas in the unstained TEM image correspond to more electron dense poly(methacrylic acid-LC) domains.

SAXS patterns obtained with x-rays incident parallel to the film surface (cross-sectional) confirm the layering of the domains parallel to the substrate surface with quite long range order (6th order reflections are readily observed). A lamellar period of 175 nm is calculated using the third and higher orders of the lamellar reflections, and is in good agreement with the period derived by the TEM inspection. Order parameters ($P_2 = \langle 3 \cos^2 \alpha - 1 \rangle / 2$, the second coefficient of the orientation distribution function) as high as 0.77 for the lamellae and 0.55 for the smectic layers were derived in the manner of Windle and Mitchell^[19] from data taken from a particularly well aligned and large-grained sample. The smectic order parameter was measured as a function of temperature. Starting from 0.29 at 40 °C, it decreased and increased reversibly by a factor of 2 on thermal cycling to 70 °C and back to 40 °C.



Figure 14a



Figure 14b

Figure 14. Photographs of pieces of the reflective polymer, field of view is 1x2 mm. The cracks were accidentally introduced during sample removal.
a. Sample at 30 °C. b. Sample at 80 °C

in the magnitude of the transmittance. However, these effects are no longer reversible – upon cooling back to 40 °C from 90 °C the minimum remained centered at 600 nm (vs. the 560 nm initial position).

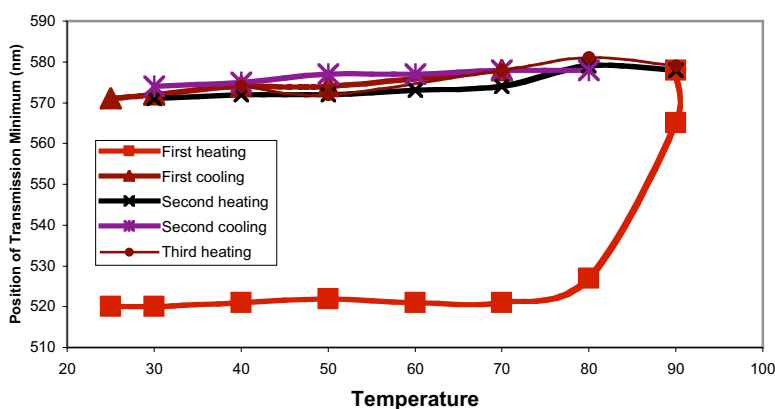


Figure 15. Position of the transmission as a function of temperature shows that a substantial change in the reflection band occurs with the smectic-to-isotropic transition; however, this change is irreversible with the existing materials.

We investigated the temperature dependence of the optical properties of this self assembled dielectric stack by obtaining the normal incidence transmission spectrum of 200 micron thick samples illuminated with an incandescent white light source through a plane polarizer using a hot stage mounted in an optical microscope with a heating and cooling rate of 10 °C /min. Heating from room temperature up into, but not beyond the transition region gave a small, reversible red-shift of the minimum of the sample transmittance (e.g., a 9 nm shift from 560nm to 569nm occurs over the interval from 40 °C to 70 °C, accompanied by a decrease in the transmitted intensity from about 72% to 60%, i.e. the sample became more reflective). Heating beyond the smectic to isotropic transition, to 90 °C, produces a substantial red-shift of 40nm in the minimum of the sample transmittance without change

The simulated normal incidence reflectance for three ideal structural states (I, IIa, IIb) is plotted in Figs. 12b and 12c. Since experimental samples exhibit layer misorientation as well as a relatively low and a temperature dependent order parameter of the mesogens, it is informative to compute the reflectance as a function of incident angle for TE and TM polarizations for suitable choices of refractive indices. Simulations of the reflectance calculated using 50 periods (corresponding to a film about 9 microns thick) for various mesogen orientations show that the case in which the index of the PS domain is matched to n_e of the PMAA-LC domain results in the material functioning as a *polarizing filter*, as TE modes within the band gap

are stopped whilst TM modes are allowed to propagate. From simulations such as these, we are able to identify relevant criteria (refractive indices, mesogen orientation, anchoring conditions and microdomain geometry) that we can use in the design of our material system to achieve particular properties.

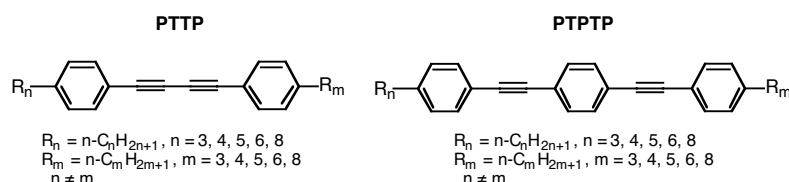
The experimental results agree qualitatively with those predicted by our simulations, which anticipate an increase in the efficiency of the stop band as observed by the deepening of the transmission dip, and a small shift of the stop band to higher wavelengths. This is expected due to the increase in index contrast between the layers. The gradual change in transmission is due to a similarly gradual transition in the order parameter of the mesogens on melting. The small, broad second heating transition centered at 78 °C and the lack of an observable exotherm on cooling suggest that the packing of the mesogens in the original “as-cast” state is quite different than in states achieved by subsequent thermal cycling of the material. The significant rate dependence of the enthalpy of the transition - e.g. cooling faster than 20 °C/min. in the DSC resulted in the absence of the peak in a subsequent heating experiment, also suggests that the reorganization of the mesogens is relatively slow. It is very likely that the morphology space accessible to the sample in the solid state is very different than that it experienced in the presence of solvent, such as when initially produced by casting. Path dependent morphologies are an important feature of liquid crystalline block copolymers^[18].

2.7 High birefringence LCs and Modeling of Orientational Interactions: University of Southern California Dalton’s research has been focused on three tasks:

1. preparation of new polar tolane liquid crystals for evaluation by Dr. Shin-Tson **Wu** of HRL Laboratories,
2. development of new theory to better understand order achieved in LC materials characterized by intermolecular electronic electrostatic interactions as well as by shape effects, and
3. attempts to achieve higher order in phase-separation LC systems by exploitation of hydrogen bonding.

The first objective has been quite successful. New nematic LC materials have been prepared with improved properties. A patent application entitled “Polar Tolane Liquid Crystals” has been prepared. The second objective has likewise been advanced. Improved theory has been developed and demonstrated for the calculation of phase diagrams. The results in the third area of activity has been interesting and unanticipated. Phase separation in ABCA’ block copolymers has been observed by electron microscopy. However, the morphology has been observed to be more complicated than anticipated.

We have synthesized a series of asymmetric diphenyl-diacetylene liquid crystals (**PTTP**), which provide a useful electro-optic medium for modulating infrared radiation and high-speed light shutters due to their high birefringence (Δn) and relatively low viscosity. In particular, these materials have been utilized for device applications by Hughes Research Laboratories and by Raytheon. Clearly, there is a need to improve the birefringence of this class of nematic LC materials leading us to develop the **PTPTP** family of LC materials.



TPTP incorporates one more phenyl group into PTTP backbone, which increased the birefringence due to the conjugation length increase of the long axis. However this modification changed the physical properties of the liquid crystals as well, such as higher

melting temperature. The asymmetric alkyl chains helped to lower melting temperature significantly. Therefore, we synthesized the PTPTP homologues with different asymmetric alkyl terminal groups to explore the highest Δn that can be obtained while keeping melting temperature with in an acceptable range. We started from PTPTP-48, -46 and -68, compounds which should give us birefringence around 0.46 in the visible region, compared to 0.40 for PTTP liquid crystal materials.

Because p-hexyl benzaldehyde or p-hexyl benzaldehyde diethyl acetal was not commercially available, We used reduction of acid chloride with lithium tri-t-butoxyaluminumhydride to produce the p-hexylbenzaldehyde. The reactions

from p-hexylbenzaldehyde to corresponding PTPTP are similar to above procedures. These materials were provided to **Wu** for characterization (see S. T. Wu, C. S. Hsu, K. F. Shyu, Y. Y. Chuang, H. B. Cheng, Z. Chai, G. Day, L. Guo and L. R. Dalton, "High Birefringence Bis-Tolane Liquid Crystals for Display Applications," *SID Tech. Digest*, **30**, 706-9, 1999). A patent has recently been filed by Hughes dealing with materials synthesized during the past two years.

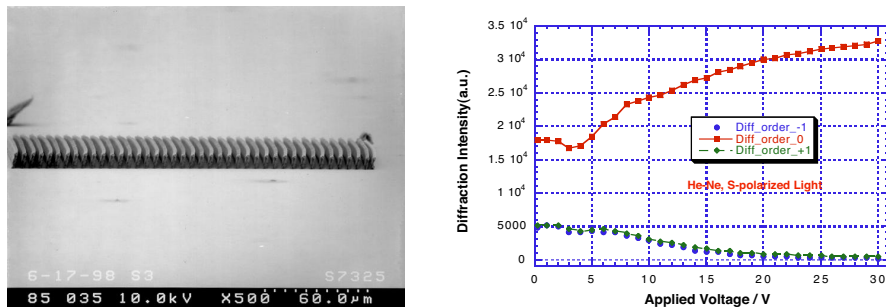


Figure 16. Left: SEM image of a single-layer 5- μm period grating. Right: 0th- and 1st-order diffracted intensity versus applied AC field (1kHz).

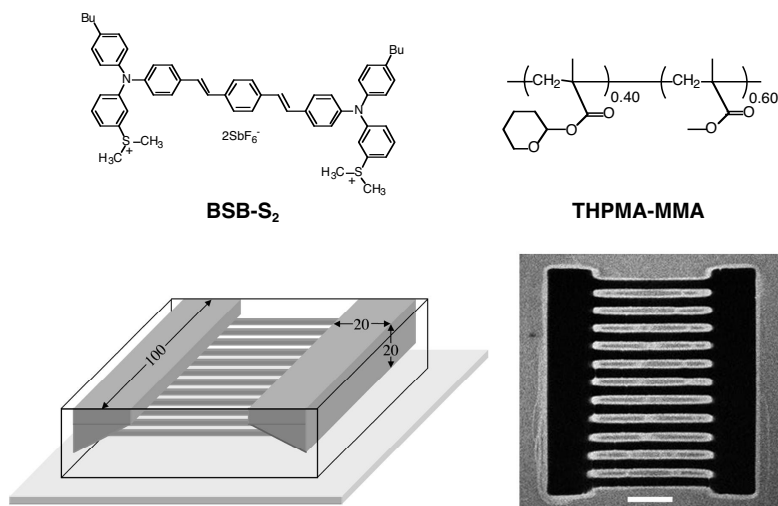


Figure 17. **BSB-S₂**: High-sensitivity two-photon photoacid generator. **THPMA-MMA**: Acid-sensitive chemically amplified resist. **Bottom left**: Schematic of a target 3D grating structure fabricated in the positive resist (dimensions are in microns). **Bottom right**: Two-photon fluorescence image-slice of the fabricated microstructure taken at a depth of 10 μm below the surface showing the buried microchannels. The scale bar corresponds to 20 μm .

microlithography for fabricating switchable microoptical devices. **Marder** and **Perry** have developed the high-sensitivity two-photon photoacid generator **BSB-S₂**, which can be used for patterning acid-sensitive materials. **Ober's** group has developed **THPMA-MMA**, a solid-state chemically amplified resist based on acid-cleavable side-chain ester groups. The initiator and polymer have been combined to form a two-photon-patternable resist and have been used for high-fidelity positive-tone 3D microfabrication of grating structures (Fig. 17).^[21] The grating channels can be back-filled with liquids, including liquid crystals. They are currently investigating the use of this material system for fabricating more complicated switchable microoptical structures.

2.8 Microfabrication of Switchable LC grating Devices: Univ. of Arizona, Kent State and Cornell

Perry, Marder, and Palffy-Muhoray, in collaboration with **Bunning** (AFRL/MLPJ), have explored the use of two-photon microlithography for fabricating electrically switchable liquid-crystal-filled gratings (LCFGs). LCFGs may be useful in several optical applications, including electro-optic switching, free-space optical interconnects, and anti-jamming. Single layer grating structures (Fig. 16) were fabricated on ITO coated substrates, treated with LC alignment layers, then packaged into cells and back-filled with 5CB and 7CB/5CB (4:1) mixtures. The packaged devices act as electrically switchable thin diffraction gratings (Fig. 16).^[20] 3D structures have also been fabricated and back-filled with LCs. Devices of this type should have application for 3-5 μm beam steering.

Perry, Marder, and Ober are also exploring the use of positive-tone 3D

3. SUMMARY

The advances in materials development under the LC MURI may play central roles in the paradigm shifts underway in display technology. Analog FLCs and new strategies for fabricating devices with the LCs that exhibit thresholdless FLC electro-optic response promise to greatly enhance the performance of FLC displays and open unprecedented FLC applications such as beam steering where analog response is vital. New electron conducting organic compounds address challenges in OLED technologies. Mirrorless lasing in cholesterics may open new strategies for control of color and directionality in emissive displays. Thermally reversible LC gels present opportunities for facile coating and control of orientation in web-based processing of LCDs and LC-based optical elements (compensators, filters and polarizers). In addition, new LCs and additives developed under the MURI are expanding the spectral range and enhancing the performance of existing LCDs. Beyond displays, the new materials, fabrication strategies and devices explored by the MURI team feed into sensor, actuator and signal processing technologies.

Bibliography

- [1] S. Bardon, D. Coleman, N.A. Clark, T. Kosa, H. Yuan, and P. Palffy-Muhoray, *Europhysics Letters*, **58**, 67-73 (2002)]
- [2] N.A. Clark, J.E. Maclellan, R. Shao, D.A Coleman, S. Bardon, T. Bellini, D.R. Link, G. Natale, M.A. Glaser, D.M. Walba, M.D. Wand, X.-H. Chen, P. Rudquist, J.P.F. Lagerwall, M. Buivydas, F. Gouda, and S.T. Lagerwall, *Materials Chemistry* **9**, 1257-1261 (1999)].
- [3] N.A. Clark, D. Coleman, and J.E. Maclellan, *Liquid Crystals* **27**, 985-990 (2000); D. Coleman, D. Mueller, N.A. Clark, J.E. Maclellan, R.F. Shao, S. Bardon, and D.M. Walba, *Physical Review Letters* (to appear 2002).]
- [4] N.A. Clark, T. Bellini, R.F. Shao, D. Coleman, S. Bardon, D.R. Link, J.E. Maclellan, X.H. Chen, M.D. Wand, D.M. Walba, P. Rudquist and S.T. Lagerwall, " *Applied Physics Letters* **80**, 4097-4099 (2002).]
- [5] D.M. Walba ,L. Xiao, P. Keller, R. Shao, D. Link, N.A. Clark, *Pure Appl. Chem.* **51**, 2117-2123 (1999).]
- [6] P. Palffy-Muhoray, T. Kosa and Weinan E, *Appl. Phys. A* **75**, 294 (2002)
- [7] S. Bardon, D. Coleman, N.A. Clark, T. Kosa, H. Yuan and P. Palffy-Muhoray, *Europhys. Lett.* **58** (1), pp. 67-73, 2002
- [8] H. Finkelmann, S.T. Kim, A. Munoz, P. Palffy-Muhoray and B. Taheri, *Adv. Mat.* 1069-1072, **13**, (2001)
- [9] N. Susa, *Japanese Journal of Applied Physics Part 1-Regular Papers Short Notes & Review Papers* **2000**, 39, 6288.
- [10] S. A. Asher, J. Holtz, J. Weissman, G. S. Pan, *Mrs Bulletin* **1998**, 23, 44.
- [11] K. Lee, S. A. Asher, *Journal of the American Chemical Society* **2000**, 122, 9534.
- [12] A. Urbas, R. Sharp, Y. Fink, E. L. Thomas, M. Xenidou, L. J. Fetters, *Advanced Materials* **2000**, 12, 812.
- [13] S. W. Leonard, J. P. Mondia, H. M. van Driel, O. Toader, S. John, K. Busch, A. Birner, U. Gosele, V. Lehmann, *Physical Review B* **2000**, 61, R2389.
- [14] K. Busch, S. John, *Physical Review Letters* **1999**, 83, 967.
- [15] Y. K. Ha, Y. C. Yang, J. E. Kim, H. Y. Park, C. S. Kee, H. Lim, J. C. Lee, *Applied Physics Letters* **2001**, 79, 15.
- [16] C. S. Kee, H. Lim, Y. K. Ha, J. E. Kim, H. Y. Park, *Physical Review B* **2001**, 6408, 5114.
- [17] D. W. Berreman, *Journal of the Optical Society of America B-Optical Physics* **1972**, 62.
- [18] C. O. Osuji, J. T. Chen, G. Mao, C. K. Ober, E. L. Thomas, *Polymer* **2000**, 41, 8897.
- [19] G. R. Mitchell, A. H. Windle, *Polymer* **1983**, 24, 285.
- [20] S. M. Kuebler, K. Mohanalingam, T. Kosa, T. Bunning, P. Palffy-Muhoray, S. R. Marder and J. W. Perry, to be published.
- [21] W. Zhou, S. M. Kuebler, K. L. Braun, T. Yu, J. K. Cammack, C. K. Ober, J. W. Perry and S. R. Marder, *Science* **2002**, 296, 1106.